Since January 2020 Elsevier has created a COVID-19 resource centre with free information in English and Mandarin on the novel coronavirus COVID-19. The COVID-19 resource centre is hosted on Elsevier Connect, the company's public news and information website.

Acta Biomaterialia 151 (2022) 491–500

Contents lists available at ScienceDirect

Acta Biomaterialia

journal homepage: www.elsevier.com/locate/actbio

Full length article

Single-injection COVID-19 subunit vaccine elicits potent immune responses

Xiaoyong Zhou[a], Haozheng Wang[a], Ying Luo[b], Lei Cui[a], Ying Guan[a,*], Yongjun Zhang[a,b,*]

[a] Key Laboratory of Functional Polymer Materials and State Key Laboratory of Medicinal Chemical Biology, Institute of Polymer Chemistry, College of Chemistry, Nankai University, Tianjin 300071, China
[b] School of Chemistry, Tiangong University, Tianjin 300387, China

ARTICLE INFO

Article history:
Received 5 May 2022
Revised 23 July 2022
Accepted 2 August 2022
Available online 7 August 2022

Keywords:
COVID-19 vaccines
Single-injection vaccines
Pulsatile release
Unconventional release kinetics

ABSTRACT

Current vaccination schedules, including COVID-19 vaccines, require multiple doses to be administered. Single injection vaccines eliciting equivalent immune response are highly desirable. Unfortunately because unconventional release kinetics are difficult to achieve it still remains a huge challenge. Herein a single-injection COVID-19 vaccine was designed using a highly programmable release system based on dynamic layer-by-layer (LBL) films. The antigen, S1 subunit of SARS-CoV-2 spike protein, was loaded in $CaCO_3$ microspheres, which were further coated with tannic acid (TA)/polyethylene glycol (PEG) LBL films. The single-injection vaccine was obtained by mixing the microspheres coated with different thickness of TA/PEG films. Because of the unique constant-rate erosion behavior of the TA/PEG coatings, this system allows for distinct multiple pulsatile release of antigen, closely mimicking the release profile of antigen in conventional multiple dose vaccines. Immunization with the single injection vaccine induces potent and persistent S1-specific humoral and cellular immune responses in mice. The sera from the vaccinated animal exhibit robust *in vitro* viral neutralization ability. More importantly, the immune response and viral inhibition induced by the single injection vaccine are as strong as that induced by the corresponding multiple dose vaccine, because they share the same antigen release profile.

Statement of significance

Vaccines are the most powerful and cost-effective weapons against infectious diseases such as COVID-19. However, current vaccination schedules, including the COVID-19 vaccines, require multiple doses to be administered. Herein a single-injection COVID-19 vaccine is designed using a highly programmable release system. This vaccine releases antigens in a pulsatile manner, closely mimicking the release pattern of antigens in conventional multiple dose vaccines. As a result, one single injection of the new vaccine induces an immune response and viral inhibition similar to that induced by the corresponding multiple-dose vaccine approach.

1. Introduction

The global COVID-19 pandemic has lasted for more than 2 years and caused over 6.0 million deaths according to Johns Hopkins University [1]. Similar to the prevention of other infectious diseases, vaccine is regarded as the best approach to contain the deadly pandemic [2–4]. Numerous COVID-19 vaccine candidates are now investigated world-wide, using different platforms including inactivated or live attenuated viruses, subunit vaccines, viral vectors, and nucleic acid [2,3]. Some of them have been authorized for emergency use and help reduce the number of hospitalizations and deaths due to COVID-19 [2]. However, for most of the COVID-19 vaccines, to achieve a long-lasting and potent protective immunity, additional booster immunizations are required [2]. For subunit vaccines this is particularly true because of their limited immunogenicity. Subunit COVID-19 vaccines have been designed using various antigens, including trimeric spike protein of the novel coronavirus [5,6], the S1 subunit of spike protein [7,8], receptor-binding domain of spike protein [9–12], etc. Even when various adjuvants, including alum [12], Freund's adjuvant (FA) [12], Toll-like receptor

* Corresponding authors at: Key Laboratory of Functional Polymer Materials and State Key Laboratory of Medicinal Chemical Biology, Institute of Polymer Chemistry, College of Chemistry, Nankai University, Tianjin 300071, China.
E-mail addresses: yingguan@nankai.edu.cn (Y. Guan), yongjunzhang@nankai.edu.cn (Y. Zhang).

https://doi.org/10.1016/j.actbio.2022.08.006
1742-7061/

9 agonist CpG [6,8], monophosphoryl lipid A for Toll-like receptor 4 [8], and cubic manganese oxide nanoparticle [9], and various delivery systems, including liposomes [8], polymersomes [6], and mesoporous silica rods [13], were used, booster immunizations were still required [2].

Replacing multiple-dose vaccines with single-dose ones will not only reduce vaccination costs, but more importantly improve the compliance and thus raise the vaccination coverage [14–16]. Particularly considering the high contagiousness of COVID-19-causing SARS-CoV-2 virus, less physician office visits reduce the possibility of being transmitted during the visits. Single-injection vaccines can be designed using controlled-release systems which allow sustained or pulsatile release of an antigen [16]. Unfortunately, because of the difficulty in achieving the unconventional release kinetics, no commercialized single injection vaccine appeared yet, despite of significant efforts made during the past four decades [15].

Compared with sustained antigen release, pulsatile release mimics the conventional vaccine schedule more closely [16], and therefore might be more safe and effective [15]. Presently most studies use poly(lactic-co-glycolic acid) (PLGA) microspheres to encapsulate antigens to achieve a delayed release [17–20]. The encapsulation process often leads to denaturation and loss of antigenicity of the antigens [20]. Distinct pulsatile release is difficult to achieve using this method. In addition the lag time is difficult to adjust [17–20].

We previously demonstrated that layer-by-layer (LBL) films assembled using dynamic bonds as driving forces, or dynamic LBL films, disintegrate in water [21,22]. In addition, the disintegration rate keeps constant if the film is assembled from monodisperse components [23]. Using them as erodible coatings time-controlled release systems with distinct pulsatile releases were designed [24,25]. The lag time can be precisely and facilely controlled by coating thickness. Herein we demonstrated that distinct multiple pulsatile release of subunit antigen, which closely mimics the release profile of the common multi-bolus regimens, can be achieved using this powerful delivery system. Then using the S1 subunit of the SARS-CoV-2 spike protein as the antigen, a single-injection COVID-19 vaccine was designed. The single injection vaccine elicits potent humoral and cellular immune responses and neutralizing antibody response against novel coronavirus. More importantly, these responses are comparable to the corresponding multiple-dose vaccines.

2. Experimental section

Materials: S1 subunit of the SARS-CoV-2 spike protein (S1), the SARS-CoV-2 Pseudovirus Neutralization Test Kit and the SARS-CoV-2 Surrogate Virus Neutralization Test Kit were obtained from GenScript. Poly(ethylene imine) (PEI, Mw 25,000), tannic acid (TA), and polyethylene glycol (PEG, Mw 10,000) were obtained from Sigma-Aldrich. Calcium chloride ($CaCl_2$, AR) was obtained from Beijing Chemical Works. Sodium carbonate (Na_2CO_3, GR) was purchased from Bohai Chemical Industry. Cyanine5 N-hydroxysuccinimide ester (Cy5-NHS ester) was obtained from MeiLunBio. Mouse granulocyte-macrophage colony stimulating factor (GM-CSF) and interleukin-4 were purchased from Abbkine (Wuhan, China). Tumor necrosis factor-α (TNF-α), interferon-γ (IFN-γ), mouse cytokine interleukin-6 (IL-6) and mouse cytokine interleukin-4 (IL-4) ELISA kits were purchased from Meimian (Jiangsu, China). Cell counting kit-8 (CCK-8) kits were purchased from Beyotime Biotechnology (China). BCA protein assay kits were provided by NJJCBIO (Nanjing, China). BSA was provided by Gentihold. Fluorescein isothiocyanate (FITC) was purchased from Solarbio. Fluorescein-labeled bovine albumin (FITC-BSA) was synthesized from FITC and BSA following the manufacturer's instructions. Cyanine5-labeled bovine albumin (Cy5-BSA) was synthesized from BSA and Cy5-NHS ester following the manufacturer's instructions.

Preparation of S1 subunit-loaded $CaCO_3$ microspheres: To prepare S1 subunit-loaded $CaCO_3$ microspheres (S1@$CaCO_3$), 1 mL of Na_2CO_3 (0.3 M) was added to 1 mL of $CaCl_2$ (0.3 M) containing 500 μg of S1 subunit. After 5 min stirring, the precipitate was centrifugated, washed with deionized water for 3 times, and freeze-dried. Other protein-loaded $CaCO_3$ microspheres, i.e., BSA@$CaCO_3$, FITC-BSA@$CaCO_3$ and Cy5-BSA@$CaCO_3$, were prepared using the same method. The loading efficiency of protein was determined using BCA protein assay kits or a RF-5301PC Shimadzu fluorescence spectroscope. The empty $CaCO_3$ microspheres were prepared using the same process but no protein was added.

Preparation of single-injection vaccine: For the preparation of the single-injection vaccines, the S1@$CaCO_3$ microspheres were first coated with TA/PEG films via layer-by-layer assembly [26]. For this purpose, TA (1 mg/mL) and PEG (1 mg/mL) solutions were prepared using phosphate buffer solution (5 mM Na_2HPO_4, 10 mM NaH_2PO_4). To assemble a prime PEI layer, S1@$CaCO_3$ was mixed with PEI (1 mg/mL), stirred at 4 °C for 7 min, and separated by centrifugation. They were then rinsed with buffer solution for 3 times. A TA layer was then deposited onto the microspheres using the similar procedure, followed by the deposition of a PEG layer. The alternative assembly cycle was repeated until the desired bilayer number was obtained. The resulting microspheres were lyophilized and named as S1@$CaCO_3$/$(TA/PEG)_x$, where "x" represents the bilayer number of TA/PEG film. Finally mixing S1@$CaCO_3$, S1@$CaCO_3$/$(TA/PEG)_{20}$ and S1 @$CaCO_3$/$(TA/PEG)_{40}$ microspheres (antigen weight 1:1:1) gave the single-injection vaccine. Other $CaCO_3$ microspheres, either loaded with protein or not, were covered with TA/PEG films similarly. A Phenom Desktop SEM was used to characterize the morphology of the particles. The sizes of the particles were measured using dynamic light scattering (BIC, USA).

Disintegration of TA/PEG coatings: To measure the disintegration kinetic of TA/PEG coatings, $CaCO_3$/$(TA/PEG)_n$ microspheres (1 mg) were added in pH7.4 0.01M phosphate buffer (5 mL) at 37 °C. The solution was completely collected for analysis at predetermined time intervals and equal volume of fresh solution was refilled. The concentration of TA in the release media was determined using a UV-2401PC Shimadzu UV-Vis spectrometer at 221 nm.

In vitro release of protein: To measure the release kinetics of protein loaded in $CaCO_3$ microspheres, 1 mg of FITC-BSA@$CaCO_3$/$(TA/PEG)_n$ microspheres were added in pH 7.4 0.01M phosphate buffer solution (5 mL) at 37 °C. At predetermined time intervals, the release solution was completely collected, followed by the addition of equal volume of fresh solution. The amount of FITC-BSA released into the media was measured using a RF-5301PC Shimadzu fluorescence spectroscope. CD spectra of the protein were acquired using a Chirascan V100 circular dichroism spectrometer.

Antigen retention and APC recruitment: The animal experiments in the study were approved by the Animal Care and Use Committee at Nankai University (No. 2022-SYDWLL-000466). To study the retention of antigen, different formulation vaccines containing the same amount of Cy5-BSA as model antigen, i.e., free protein, free protein + Alum and protein@$CaCO_3$, were injected subcutaneously into the hind neck of mice (C57BL/6, female, 6–8 weeks old, $n = 6$). At predetermined time intervals, the fluorescence images of mice were captured using a Lumina II IVIS® Spectrum system at 640 nm excitation wavelength. Before imaging, the mice were anesthetized by inhalation with 3% isoflurane. To study the recruitment of APCs, the subcutaneous adipose tissues near the injection sites were collected at the 48 h post injection. The infiltration of APCs was evaluated by hematoxylin and eosin staining (H&E).

In vivo release of protein: Various formulations with the same dose of Cy5-BSA, including free Cy5-BSA, Cy5-BSA@$CaCO_3$, Cy5-BSA@$CaCO_3$/$(TA/PEG)_{20}$, Cy5-BSA@$CaCO_3$/$(TA/PEG)_{40}$ and Cy5-BSA@$CaCO_3$+ Cy5-BSA@$CaCO_3$/$(TA/PEG)_{20}$ + Cy5-BSA@$CaCO_3$/$(TA/PEG)_{40}$, were injected subcutaneously into the hind neck of mice (C57BL/6, female, 6–8 weeks old, $n = 6$). At the predetermined time intervals, the mice were anesthetized and their fluorescence images were captured.

In vitro activation of BMDCs: From femurs and tibias of mice (C57BL/6, male, 3–5 weeks old) BMDCs were separated. After 2 min treatment at room temperature with Solarbio RBC lysis buffer and twice washing with RPMI 1640, the cells were cultured at 37 °C and 5% CO_2 in the RPMI 1640 complete medium containing 10% fatal bovine serum (FBS), 1% antibiotics (P/S), 5 ng/mL IL-4 and 10 ng/mL GM-CSF. Every 2 days the culture media were half-changed. The non-adherent and loosely adherent cells were collected after 8 days culture. For BMDC activation, the cells were seeded in 6-well plates with a cell density of 1×10^6 cells per well and cultured for 12 h. Then free BSA, BSA + Alum or BSA @$CaCO_3$ (2 μg BSA per well) was added, followed by additional 24 h culture. A group as negative control was treated with medium alone. Another group as positive control was treated with 1.0 μg/mL LPS. After 30 min labelling at 4 °C with FITC anti-CD80 antibody and PE anti-CD40 antibody, the cells were analyzed using a FACS Calibar flow cytometer. The mean fluorescence intensities (MFI) of the samples were normalized to that of the negative control. The cytokine levels in the supernatants were measured with ELISA Kits.

Immunization: 5 groups of mice (C57BL/6, female, 6–8 weeks old) with 6 mice per group were involved in the study. The PBS, 3 × S1, 3 × S1+Alum, 3 × S1@$CaCO_3$ group received three injections of PBS, free S1 subunit, S1 subunit with Alum and S1 subunit@$CaCO_3$, respectively, at an interval of 14 days. For the Single injection vaccine group, only one injection of the single-injection vaccine (S1@$CaCO_3$ +S1@$CaCO_3$/(TA/PEG) $_{20}$ +S1@$CaCO_3$/$(TA/PEG)_{40}$) was received. Expect for PBS control group, for all the groups the total dose of S1 subunit was 24 μg. Every 7 days sera were collected. The concentrations of the specific antibodies were determined using a SARS-CoV-2(2019-nCoV) Spike S1 Antibody Titer Assay ELISA kit (mouse). To follow the growth of the mice, their weight was measured twice a week. To evaluate the biosafety of the single-injection vaccine system, the animals were sacrificed 42 days post immunization. The tissues of heart, lung, spleen, liver, and kidney were collected, and stained with H&E.

In vitro re-stimulation of splenocytes: From the immunized mice the splenocytes were collected by grinding the spleens through a 200 mesh cell filter and splitting the erythrocytes 42 days post immunization. After PBS washing, the splenocytes were cultured in RPMI 1640 complete medium supplied with 1% P/S, 10% FBS, and 5 μg/mL S1 subunit. After 72 h culture, the cell viability was assayed using CCK-8. The concentrations of cytokines (IFN-γ, TNF-α, IL-4, and IL-6) in the supernatants (collected after 24 h re-stimulation) were determined using ELISA Kits. To detect effector memory T cells, the cells were analyzed with a flow cytometer (BD, USA) after labeled with PE anti-CD8 antibody, FITC anti-CD4 antibody, and APC anti-CD69 antibody.

SARS-CoV-2 surrogate virus neutralization test: SARS-CoV-2 surrogate virus neutralization test kit (GenScript) was used to perform SARS-CoV-2 surrogate virus neutralization test. The manufacturer's protocols were followed. Briefly, using sample dilution buffer the serum samples were diluted 1:100. After adding equal volume of HRP-RBD solution, the mixture was incubated at 37°C for 30 min. It was then added to wells precoated with ACE2 protein. After 15 min incubation at 37 °C, the plate was washed four times, followed by adding 100 μL of TMB solution to each well and 15 min incubation in the dark at 25 °C. Finally, by adding the stop solution, the reaction was terminated, and the absorbance at 450 nm was recorded. Inhibition of RBD-ACE2 binding was calculated according to the following equation:

$$\text{Inhibition} = \left(1 - \frac{OD\ Value\ of\ Sample}{OD\ Value\ of\ Negative\ Control}\right) \times 100\% \quad (1)$$

SARS-CoV-2 pseudovirus neutralization test: SARS-CoV-2 pseudovirus neutralization test was performed using the SARS-CoV-2 pseudovirus neutralization test kit from GenScript following the manufacturer's protocols. Briefly, the sera were collected from the immunized mice and inactivated for 30 min at 56 °C. The treated sera were diluted in proportion, mixed with SARS-CoV-2 pseudovirus and incubated for 1 h. The mixtures were then added to a dispersion containing 6×10^5 Opti-HEK293/ACE2 cells. After incubated at 37 °C for 48 h, firefly luciferase test agent (GenScript) was added. The fluorescence signal values were read using Microplate Reader (Biotek, USA). The infection degree was evaluated by using the formula:

$$\text{Inhibition} = \left(1 - \frac{Value\ of\ Positive\ Control - Value\ of\ Blank\ Control}{Value\ of\ Negative\ Control - Value\ of\ Blank\ Control}\right) \times 100\% \quad (2)$$

Cytotoxicity: In the 96-well plates BMDCs cells were seeded at a density of 1×10^5 cells per well, followed by adding RPMI 1640 medium containing 10% FBS, 1%PS and various concentrations of $CaCO_3$/$(TA/PEG)_{40}$ microspheres (25, 50, 75,100 and 125 μg/mL). After 24 h culture, CCK-8 reagent (10 μL) was added into the wells. After 3 h incubation, using a Tecan Spark microplate reader the absorbance at 450 nm was determined. The cell viability, i.e., the ratio of the absorbance values of the wells containing microspheres and the negative control wells without microspheres, was calculated.

Statistical analysis: The experimental data were reported as means ± standard deviation. Statistical analysis was carried out using one-way ANOVA and indicated using $*$ for $p < 0.05$, $**$ for < 0.01 and $***$ for < 0.001.

3. Results and discussion

3.1. Synthesis of antigen-loaded microspheres

The synthesis of single-injection subunit COVID-19 vaccine using S1 subunit of the spike protein (S1) as antigen was schematically shown in Fig. 1A. First $CaCO_3$ microspheres loaded with S1 subunit were synthesized by mixing Na_2CO_3 and $CaCl_2$ in the presence of S1. The coprecipitation method has been proved an efficient method to encapsulate proteins in $CaCO_3$ microspheres [27]. To coat the $CaCO_3$ microspheres with tannic acid (TA)/polyethylene glycol (PEG) films, a primer PEI layer was first deposited, followed by layer-by-layer deposition of TA and PEG layers [26]. The film thickness could be facilely controlled by the number of deposition cycles. In this way S1-loaded $CaCO_3$ microspheres coated with various thickness of TA/PEG films were produced. Single-injection COVID-19 vaccine was obtained by simple mixing them.

Because of the high price of S1 subunit, we used a model protein antigen, BSA, to study the preparation process. As shown in Fig. 1B, the empty $CaCO_3$ microparticles are spherical with an average diameter of ~3.43 μm (Fig. 1E). Similar morphology and size were found for the BSA-loaded particles (Fig. 1C and F). The loading efficiency was determined to be ~60%. The particles remain to be spherical after being further coated with TA/PEG films, however, the surface becomes less rough (Figs. 1D and S1). The successful film deposition was further demonstrated by the reversal of surface charge. Before LBL coating, the particles exhibit a negative Zeta potential. The deposition of a PEI layer reverses it to be

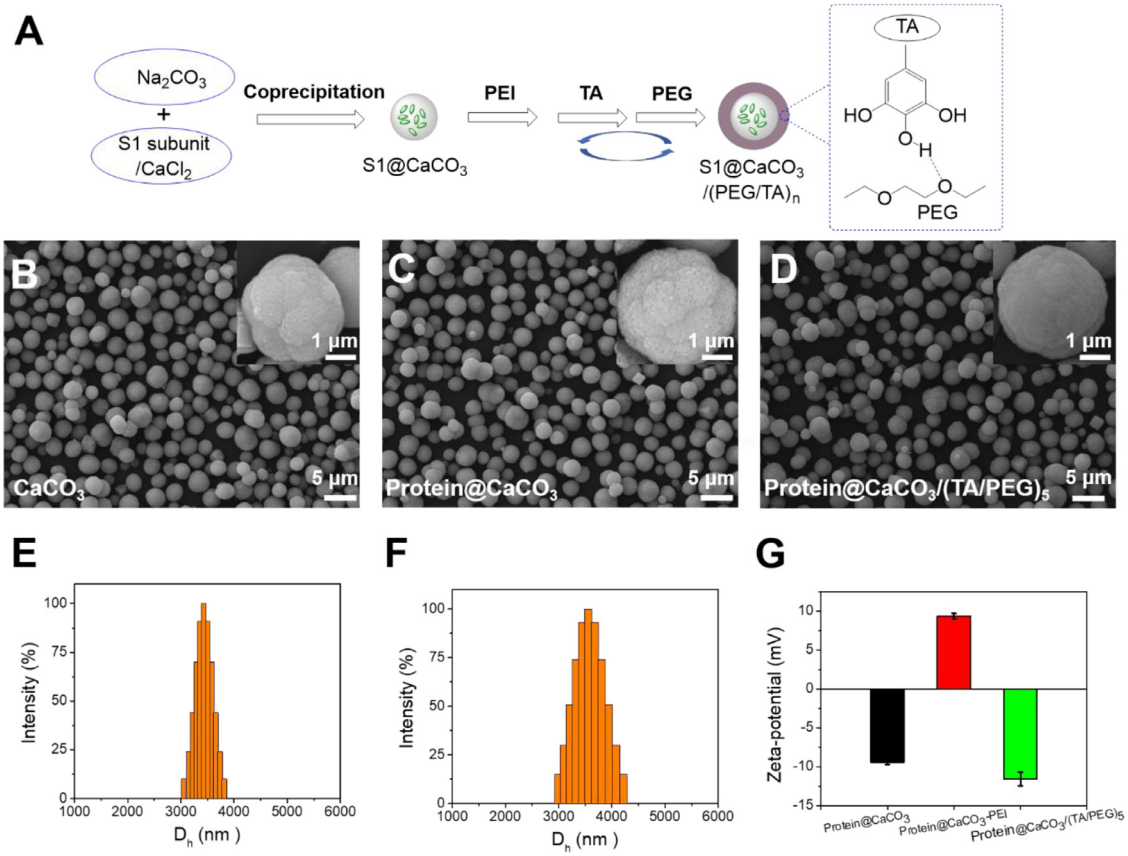

Fig. 1. (A) Encapsulation of S1 subunit in $CaCO_3$ microspheres, followed by coating with TA/PEG films by LBL assembly. (B-D) SEM images of the empty $CaCO_3$ microspheres (B), BSA@$CaCO_3$ microspheres (C) and BSA@$CaCO_3$/$(TA/PEG)_5$ microspheres (D). (E, F) Size distribution of empty $CaCO_3$ (E) and the BSA@$CaCO_3$ (F) microspheres determined using dynamic light scattering (DLS). (G) Zeta potential of BSA@$CaCO_3$ microspheres, the same microspheres deposited sequentially with a PEI layer and a 5 bilayer TA/PEG film.

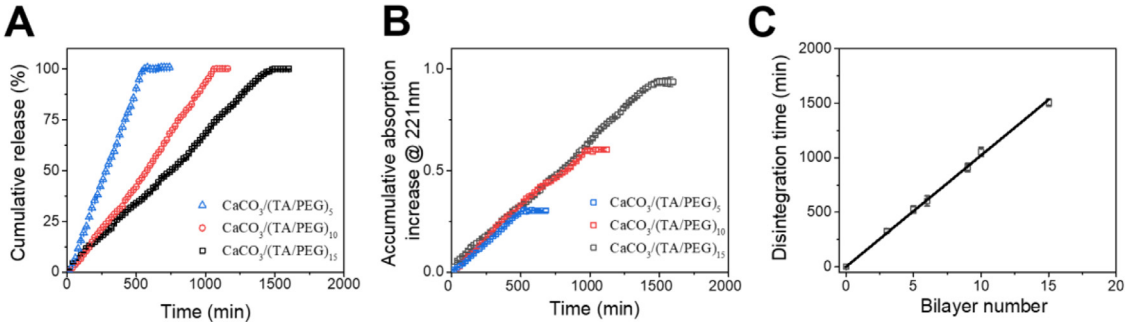

Fig. 2. (A) Release kinetics of TA from TA/PEG films-coated $CaCO_3$ microspheres plotted as cumulative release percentage. (B) Release kinetics of TA from TA/PEG films-coated $CaCO_3$ microspheres plotted as accumulative released amount of TA (denoted by accumulative adsorption increase at 221 nm). (C) Disintegration time of the TA/PEG films with different bilayer numbers.

positive, but further deposition of TA/PEG films reverses it to be negative again (Fig. 1G).

3.2. Release kinetics of protein antigen

The disintegration of TA/PEG films on $CaCO_3$ microspheres was studied by following the release of TA from the coatings into the solution. For all samples, the amount of TA released into the media increases linearly with time, indicating a constant-rate disintegration of the films (Fig. 2A). The release rate in terms of TA amount is the same for all the samples (Fig. 2B). Therefore the time required for complete disintegration of the film increases linearly with the film thickness (Fig. 2C). Adding fetal bovine serum into the media does not change the release profiles, suggesting negligible effect of proteins on the disintegration of TA/PEG films (Fig. S2). The unique behavior of TA/PEG films was previously explained [28]. Simply, because TA and PEG are bonded with hydrogen bonds, which are reversible and dynamic, the TA/PEG films disintegrate slowly when soaked in water [28]. Similar gradual disintegration behaviors were also observed for other LBL films assembled using reversible, dynamic interactions as driving forces [21–25]. The disintegration of the film is actually the dissociation of TA/PEG complex in the film. The disintegration rate, R, under the experimental conditions can be written as:

$$R = k_1[TA/PEG] \quad (3)$$

The concentration of TA/PEG complex is constant because it is a solid-like material. In addition, since both TA and PEG have a nar-

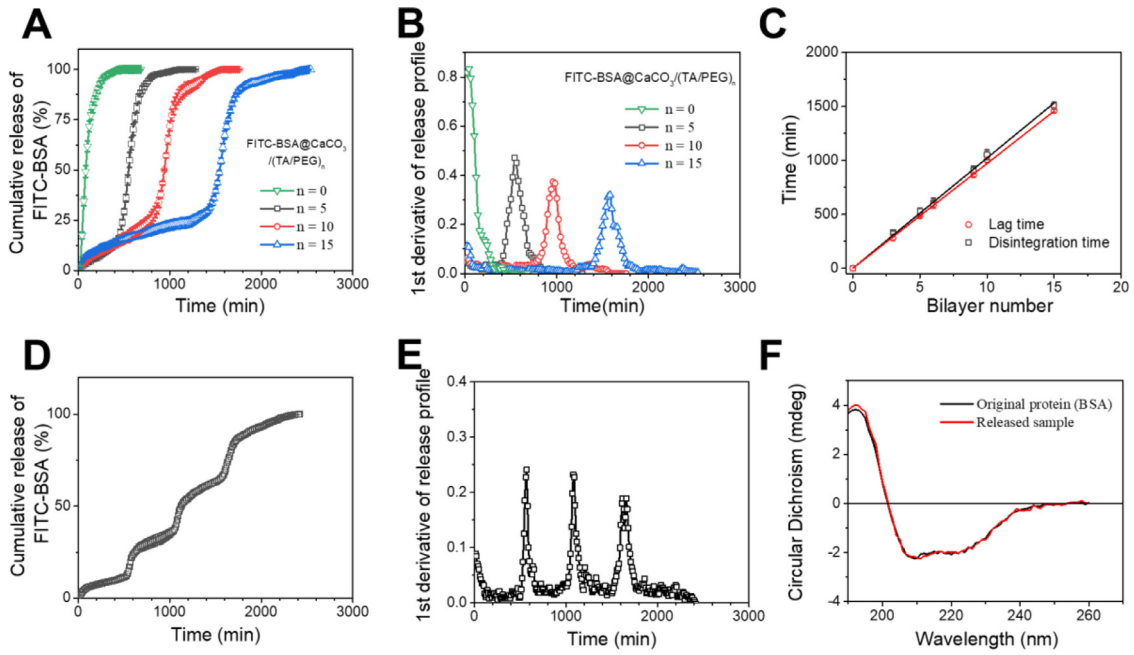

Fig. 3. (A) Release kinetics of FITC-BSA from TA/PEG films-coated FITC-BSA@$CaCO_3$ microspheres. (B) 1st derivative of the release profiles. (C) Disintegration time and lag time as a function of bilayer number of the TA/PEG coatings, respectively. (D) Release profile of FITC-BSA from a mixture of FITC-BSA@$CaCO_3$/$(TA/PEG)_5$, FITC-BSA@$CaCO_3$/$(TA/PEG)_{10}$ and FITC-BSA@$CaCO_3$/$(TA/PEG)_{15}$. (E) 1st derivative of the release profile. (F) CD spectra of the pristine BSA and BSA released from BSA/$CaCO_3$/$(TA/PEG)_{15}$.

row molecular weight distribution, k_1 could be regarded as constant. Therefore, disintegration rate of the film is constant [23,29–33].

The unique disintegration behavior of TA/PEG film makes it an ideal erodible coating for delayed drug release systems [24]. As a demonstration, FITC-BSA were encapsulated in bare and TA/PEG film-coated $CaCO_3$ microspheres. When the bare particles were put into a solution, a burst release of FITC-BSA was observed immediately. In contrast, a delayed release of FITC-BSA was observed for the TA/PEG films-coated particles (Fig. 3A). The release of FITC-BSA is prevented by the TA/PEG coating until the coating is fully disintegrated. The delayed release of FITC-BSA can also be demonstrated by the 1st derivative of the release profiles (Fig. 3B). The lag time increases linearly with the film bilayer number (Fig. 3C), suggesting it can be precisely controlled by the number of assembly cycles. Indeed, the lag time and the corresponding disintegration time of the TA/PEG coating are equal, clearly demonstrating that the release of FITC-BSA is controlled by the erosion of the coating (Fig. 3C). A single injection vaccine requires more than one pulsatile releases of the antigen. This can be accomplished simply by mixing $CaCO_3$ microspheres covered with different thickness TA/PEG films (Fig. 3D and E) [25]. The release profile comprising distinct pulsatile releases mimics closely that in prime-boost vaccination regime. In addition, as indicated by CD spectra, the secondary structure of the protein released from the microspheres remains almost intact (Fig. 3F). This property is highly desirable for a carrier when used for the encapsulation and release of protein antigens.

To study the *in vivo* release pattern of the microspheres, Cy5-BSA was chosen as a model subunit antigen. Compared with free protein, encapsulation in $CaCO_3$ microspheres significantly prolongs its retention at the injection sites from less than 24 h to 10∼13 days (Fig. 4A and B). The protein started to be released from the bare $CaCO_3$ microspheres immediately once injected (Fig. 4B). In contrast, it is delayed when the microspheres were coated with TA/PEG films (Fig. 4C and D). The lag time was 14 and 28 days for the particles covered by 20 and 40 bilayer films, respectively. For the mixed sample of three particles, i.e., Cy5-BSA@$CaCO_3$+Cy5-BSA@$CaCO_3$/$(TA/PEG)_{20}$ +Cy5-BSA@$CaCO_3$/$(TA/PEG)_{40}$, three fluorescence signal maxima were observed on Day 0, 14 and 28, indicating three pulsatile releases of Cy5-BSA (Fig. 4E). Obviously the three pulsatile releases should be attributed to the release from the bare microspheres, the microspheres covered with 20 and 40 bilayer TA/PEG films, respectively.

3.3. Humoral immune response

After establishing that the TA/PEG coated $CaCO_3$ system can achieve multiple pulsatile release of protein, a single-injection COVID-19 vaccine, i.e., S1@$CaCO_3$+ S1@$CaCO_3$/$(TA/PEG)_{20}$ + S1@$CaCO_3$/$(TA/PEG)_{40}$, was prepared by encapsulating S1 subunit, which was purchased from a commercial vendor, in the same way with BSA. The immune response of the vaccine was studied using C57BL/6 mice. For comparison, 4 groups of mice were received three injections of PBS, S1, S1 +Alum, or S1@$CaCO_3$, on Day 0, Day 14, and Day 28, respectively (Fig. 5A). Expect for the PBS control group, the total dosage of S1 of the vaccine groups was all the same (24 μg).

IgM is the first antibody produced in response to antigen invasion and the prime mediator of the primary immune response. The IgM responses induced by the vaccines were shown in Fig. 5B. For the PBS control group, over the 42-day study period no antibody response was detected, while in groups immunized with the S1 subunit-based vaccines IgM titers were detected. Among all vaccines, free S1 elicits the lowest IgM response, suggesting a weak immunogenicity of the subunit antigen. Addition of Alum adjuvant effectively improves the immune response of S1. Interestingly encapsulation of S1 in $CaCO_3$ microspheres elicits an even stronger IgM response than the S1+Alum group. One reason for the result may be that encapsulation in $CaCO_3$ microspheres leads to an even longer antigen retention at the injection site than addition of Alum adjuvant (Fig. S3) and a prolonged exposure of antigen is favourable to induce a stronger and more persistent antibody response [16]. In addition, $CaCO_3$ microspheres can recruit more APCs to the injection site than Alum adjuvant (Fig. S4). We

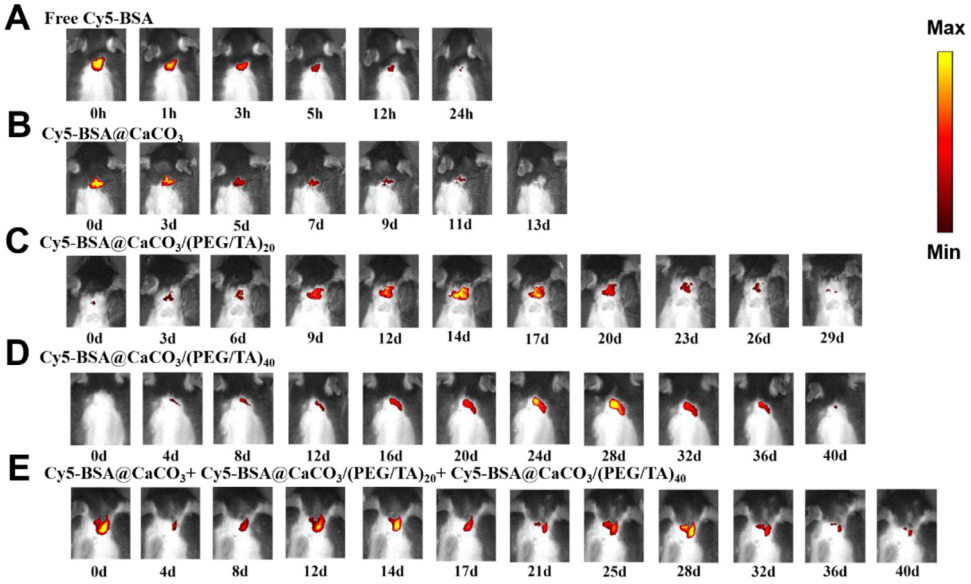

Fig. 4. Representative fluorescence images of C57BL/6 mice after receiving one administration of free Cy5-BSA (A), Cy5-BSA@$CaCO_3$ (B), Cy5-BSA@$CaCO_3$/$(TA/PEG)_{20}$ (C), Cy5-BSA@$CaCO_3$/$(TA/PEG)_{40}$ (D), and a mixture of Cy5-BSA@$CaCO_3$, Cy5-BSA@$CaCO_3$/$(TA/PEG)_{20}$ and Cy5-BSA@$CaCO_3$/$(TA/PEG)_{40}$ (E).

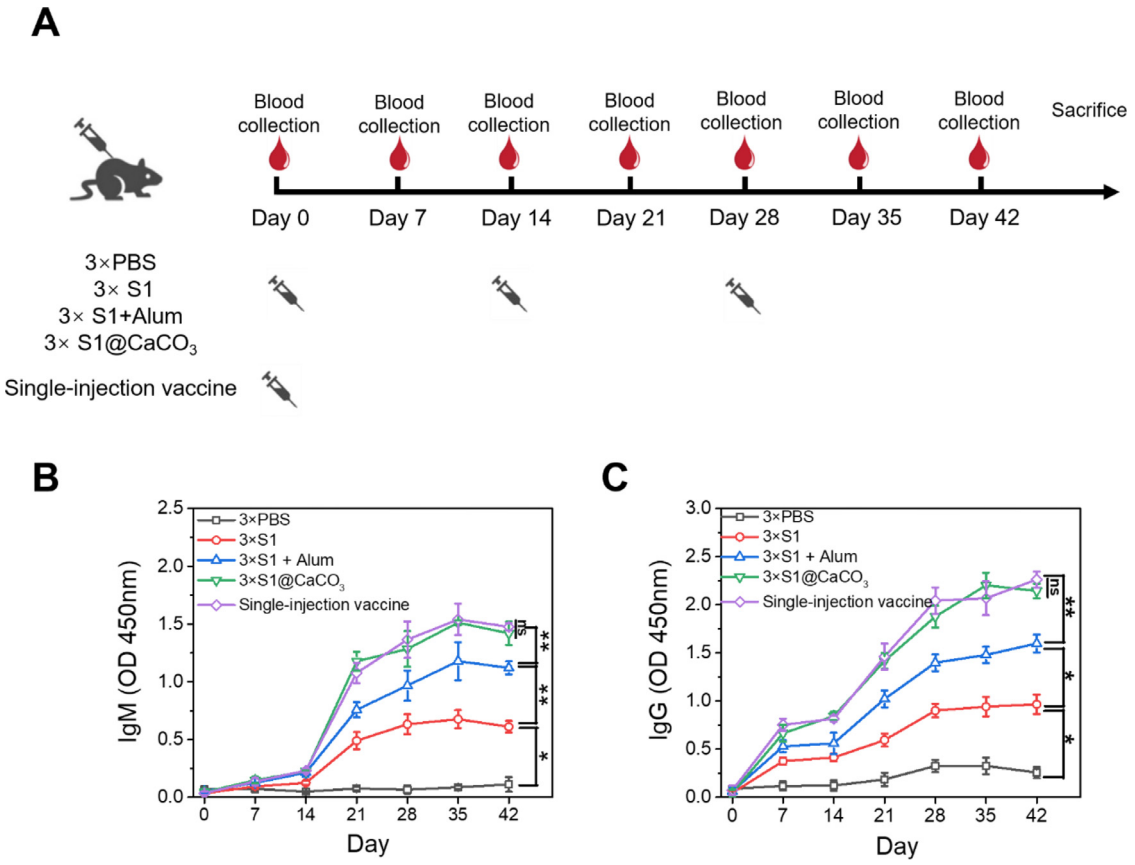

Fig. 5. Humoral immune response of the vaccines. (A) The schedule of vaccine immunization and blood collection. The single injection vaccine group receives one injection, while other groups receive three injection on Day 0, Day 14 and Day 28. (B, C) S1 subunit-specific IgM (B) and IgG (C) produced in sera of the immunized mice.

also demonstrated that encapsulation in $CaCO_3$ microspheres significantly enhances the ability of an antigen to active dendritic cells (DCs), which are widely present in the skin [34] and play a key role in immune responses. When co-incubating DCs with an antigen, compared with the Alum-adjuvanted antigen, the expression of the co-stimulatory molecule (CD40 and CD80) induced by $CaCO_3$-encapsulated antigen is significantly up-regulated (Fig. S5A-S5D). $CaCO_3$-encapsulated antigen also induces a higher level expression of cytokines (IFN-γ and IL-6) than antigen with Alum adjuvant (Fig. S5E-S5F) [35]. Fig. 5B also shows that a low level IgM response was induced by the first dose of S1, S1+Alum, and S1@$CaCO_3$. However, the IgM titers increase dramatically after the first boost, and continue to increase after the second boost. The result strongly suggests that to achieve potent, long-term protection

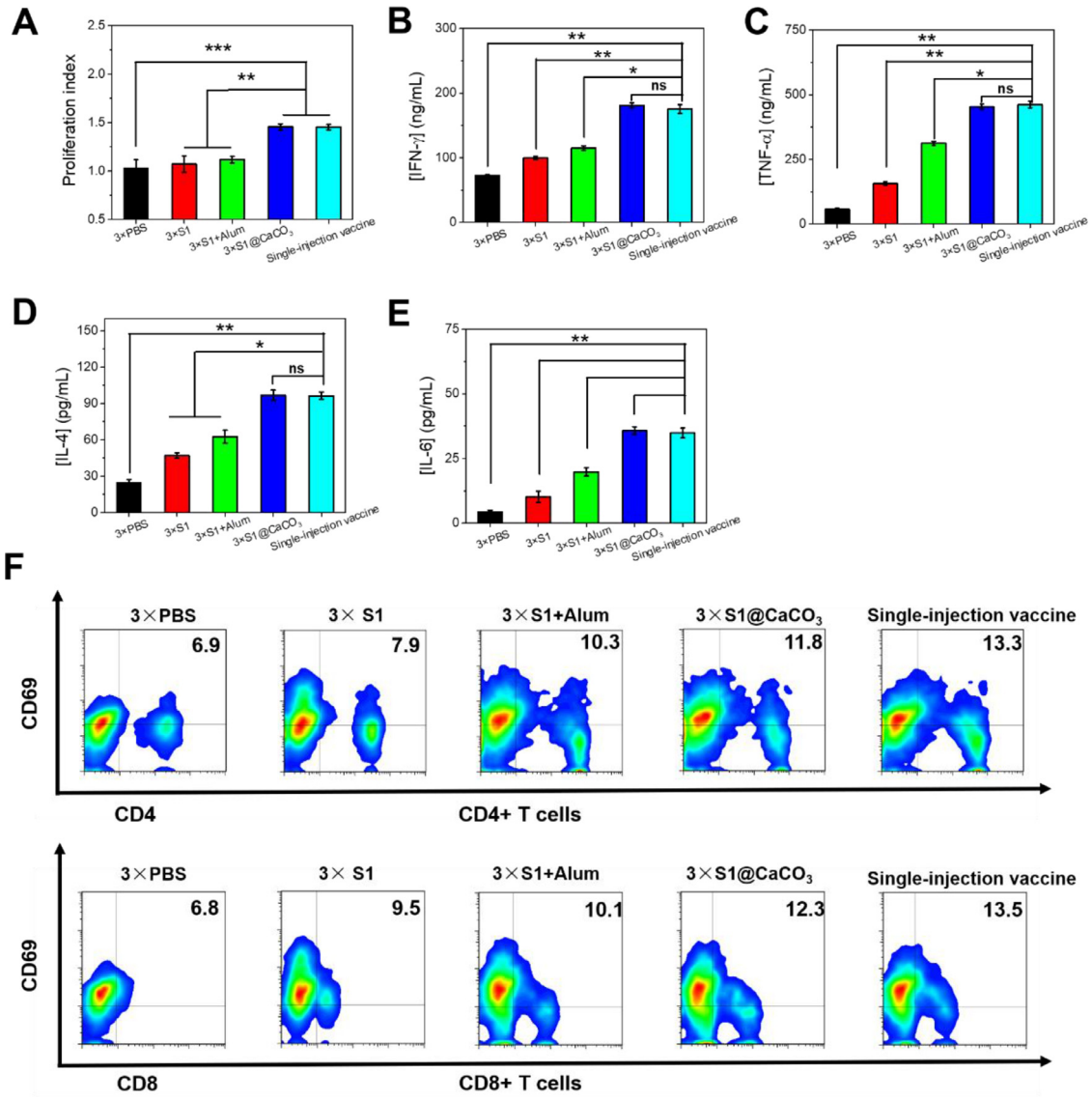

Fig. 6. Cellular immune response of the vaccines. (A) Proliferation index of splenocytes after 72 h re-stimulation with S1 subunit. (B-E) Cytokine (IFN-γ (B) and TNF-α (C), IL-4 (D), and IL-6 (E)), secretion by splenocytes after 24 h re-stimulation with S1 subunit. The cytokine concentrations in the supernatant were measured by ELISA. (F) Flow cytometry analysis of $CD4^+$ and $CD8^+$ T cells.

against the disease, boost vaccination is indispensable even when adjuvant is used. In contrast, a level of IgM titer equal to that of the 3 × S1@$CaCO_3$ group was induced in the single injection vaccine group, although only one injection was received by the group. In addition, the IgM titer increases with time in the same pattern with that of 3 × S1@$CaCO_3$ group. These results can be explained by the fact that the releasing pattern of S1 in the single injection vaccine group (three pulsatile releases on Days 0, 14, and 28, as shown in Fig. 5A) is similar to that in the 3 × S1@$CaCO_3$ group (three injections on Days 0, 14, and 28).

IgG is a key player in the humoral immune response. From Fig. 5C, the vaccine-induced IgG response follows a similar trend to IgM response. Again S1@$CaCO_3$ induced a stronger IgG response than free S1 and S1 +Alum. More importantly for the single injection vaccine group, the IgG titer increases with time in the same way with the 3 × S1@$CaCO_3$ group. Actually the IgG titer at all time points is equal to that of the 3 × S1@$CaCO_3$ group, confirming again the single injection vaccine elicits equal humoral immune response with the 3 × S1@$CaCO_3$ group.

3.4. Cellular immune responses

To evaluate cellular immune responses elicited by the vaccines, on Day 42 post immunization the mice were sacrificed. The splenocytes were collected and re-stimulated with S1 for 72 h. The low proliferation index for the free S1 group and the S1+Alum group suggests a low level activation of the splenic lymphocytes in these groups, leading to a low response when the cells were re-stimulated with the same antigen (Fig. 6A) [35]. Previously other authors also reported that S1 subunit adjuvanted with Alum elicits only humoral immunity [8]. In contrast, the 3 × S1@$CaCO_3$ group and the single injection vaccine group exhibit a high proliferation index, revealing effective activation of the splenic lymphocytes in the groups. The enhanced cellular immune response may be attributed to a significantly prolonged stimulation provided by $CaCO_3$ microspheres [16]. Note the proliferation indexes of the two groups are equal, suggesting the same level of cellular immune response is elicited by the two groups. By assaying cytokine concentration in the supernatant by ELISA, the vaccine-induced adaptive

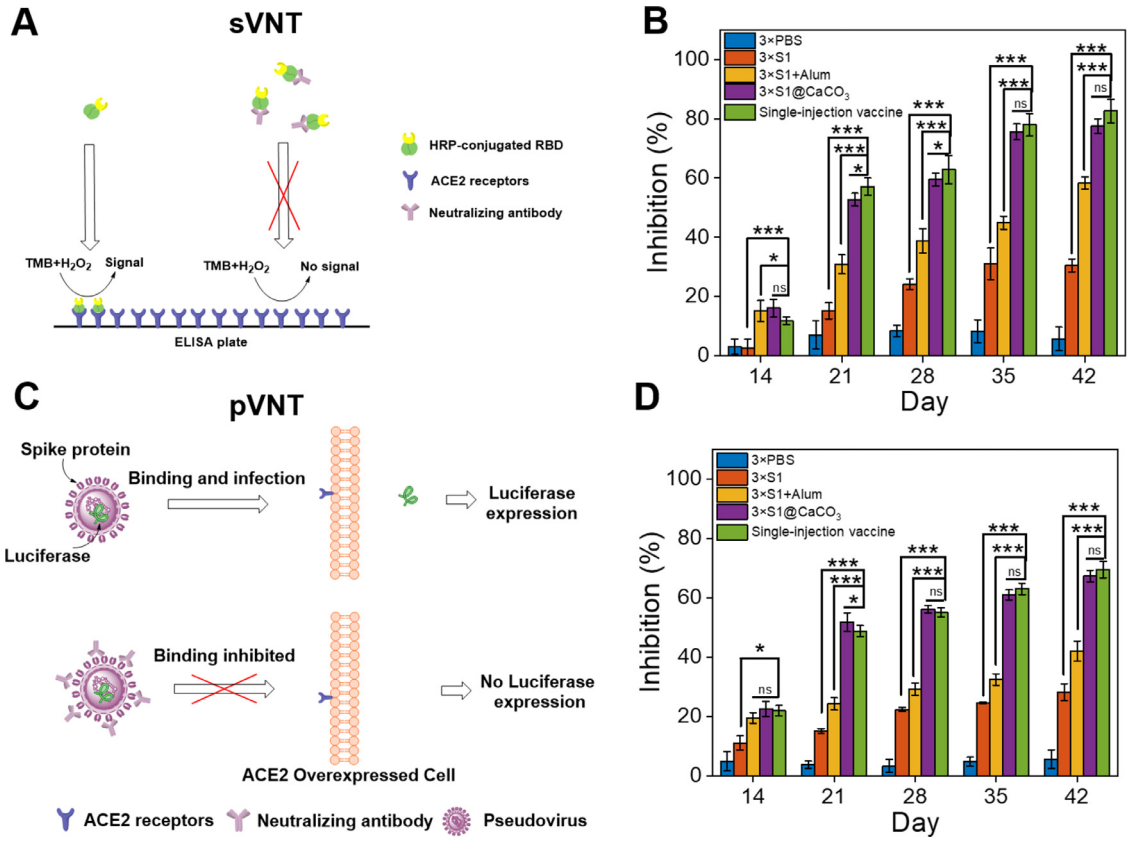

Fig. 7. (A, C) Schematic description of surrogate virus neutralization test (sVNT) (A) and pseudovirus virus neutralization test (pVNT) (C). (B, D) Inhibition of the sera from different groups measured by sVNT (B) or pVNT (D). The sera were 100-fold diluted.

T cell responses was evaluated (Fig. 6B-E). Again a more significantly up-regulated expression of the cytokines, such as TNF-α, IFN-γ, IL-4 and IL-6, was observed for 3 × S1@$CaCO_3$ group and single injection vaccine group than 3 × S1 group and 3 × S1+Alum group. Secretion of cytokines is an important way for T cells to mediate their effector function [36]. The up-regulated expression of the cytokines in 3 × S1@$CaCO_3$ group and single injection vaccine group than 3 × S1 group indicates higher vaccine-induced cell effector populations. The activation of lymphocytes was also evaluated using CD4, CD8 and CD69, the activation markers on the surface of effector immune cells (Fig. 6F). The higher ratio of $CD4^+$ and $CD8^+$ T cells of 3 × S1@$CaCO_3$ group than 3 × S1 group and 3 × S1+Alum group indicates significantly enhanced activation of lymphocytes in the group. The ratio of $CD4^+/CD8^+$ T cells for the single injection vaccine group is even higher, suggesting a more effective activation of effector immune cells in the group.

3.5. Virus neutralization tests

To study if the vaccines can inhibit viral infection, two virus neutralization tests, i.e., a surrogate virus neutralization test (sVNT) and a pseudovirus neutralization test (pVNT), were carried out. In the sVNT assay, the binding of HRP-conjugated RBD protein with the hACE2 protein pre-coated on an ELISA plate will be inhibited because the neutralizing antibody in the serum will bind with it (Fig. 7A) [37]. The inhibition measured by this test increases with time for all groups expect the PBS control, indicating the amount of neutralizing antibody increases with time during the vaccination process (Fig. 7B). Again immunization with 3 × S1@$CaCO_3$ achieves a higher inhibition than 3 × S1 and 3 × S1+Alum. More importantly the inhibition of the single injection vaccine group is equal to or slightly higher than the 3 × S1@$CaCO_3$ group. On Day 42, the inhibition achieved by 100-fold diluted serum samples is 30%, 58%, 77% and 82%, for 3 × S1, 3 × S1+Alum, 3 × S1@$CaCO_3$ and single injection vaccine group, respectively.

In pVNT, cells that express the ACE2 receptor can be infected by the pseudovirus, i.e., lentiviral particles with Spike on their surface, and the infected cells will express luciferase, a marker protein. Neutralizing antibody from the serum can bind with the surface Spike, thus inhibit the infection of the cells (Fig. 7C). Again for all vaccines, the inhibition measured by this test increases with time, suggesting increasing level of neutralizing antibody. The inhibitions achieved by the single injection vaccine group and the 3 × S1@$CaCO_3$ group are comparable, both of which are much higher than that of 3 × S1 and 3 × S1+Alum (Fig. 7D). The inhibition on Day 42 achieved by 100-fold diluted serum samples is 28%, 42%, 67% and 69%, for 3 × S1, 3 × S1+Alum, 3 × S1@$CaCO_3$ and single injection vaccine, respectively. Inhibition rates at other dilution times were also determined (Fig. S6). From these data, the IC50 value, i.e., serum dilution capable of realizing 50% inhibition, on Day 42 was determined to be 10, 560, 720 for 3 × S1+Alum, 3 × S1@$CaCO_3$ and single injection vaccine group, respectively.

3.6. Biocompatibility and biosafety

Finally the biocompatibility and biosafety of this system were evaluated. Coculture of BMDCs with TA/PEG-coated $CaCO_3$ particles does not reduce the viability of the cells, suggesting high biocompatibility of the delivery system (Fig. 8A). After immunized with the vaccines, the body weights of the animals increases steadily, indicating the vaccines, including the single injection vaccine, does not impact the mice growth (Fig. 8B). Histological analysis by H&E

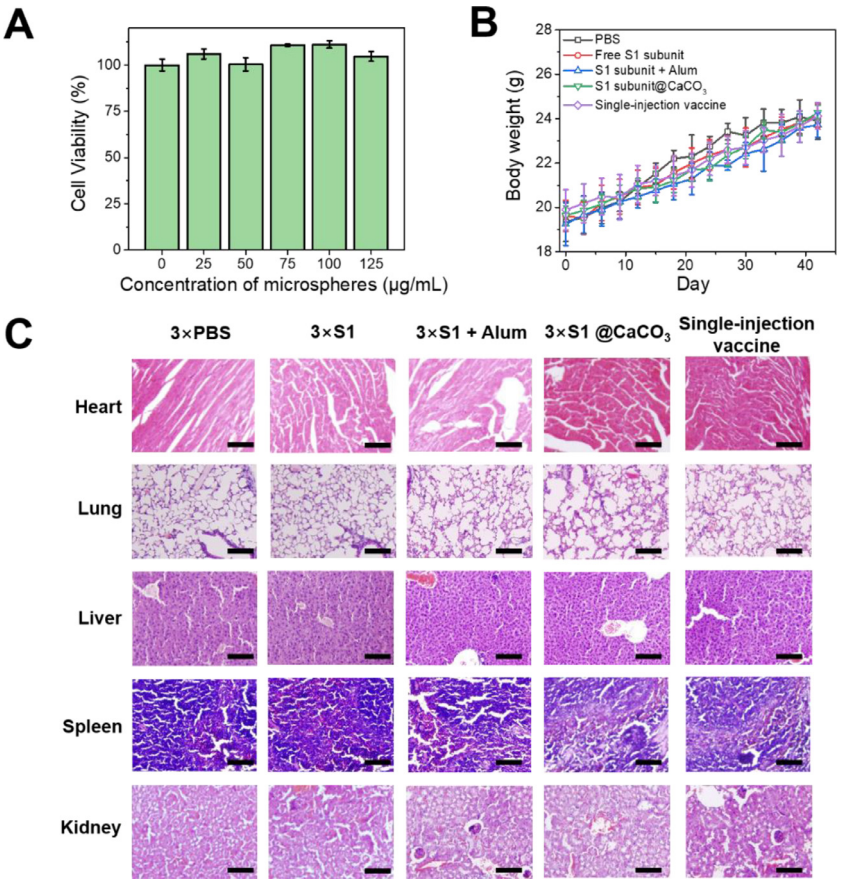

Fig. 8. (A) Viability of BMDCs after 24 h coculture with $CaCO_3$/$(TA/PEG)_{40}$ microspheres. (B) Body weights of the immunized mice changing with time. (C) H&E stained tissues of major organs harvested from immunized mice 6 weeks post-vaccination. Scale bar: 100 μm.

staining reveals that no inflammation infiltration or obvious damage in the major organs, including liver, heart, lung, spleen, and kidney (Fig. 8C). All these results suggest good biocompatibility and biosafety of the vaccines.

4. Conclusion

In summary, using a highly programmable protein release system a single-injection COVID-19 vaccine was successfully designed. Using a model protein antigen, it was confirmed that delayed release of protein antigen can be accomplished by first encapsulation of the protein antigen in $CaCO_3$ microspheres and then coating with TA/PEG films. Because the erosion rate of TA/PEG coating is constant, the lag time can be finely controlled. Multiple pulsatile releases can be facilely accomplished by mixing the protein-loaded particles covered with different thickness of TA/PEG coatings. COVID-19 vaccine was then prepared by encapsulating S1 subunit of novel coronavirus Spike protein in the release system. The single injection vaccine elicits both humoral and cellular immune responses, both of which are as potent as that induced by the corresponding multiple dose vaccine, because the antigen release pattern of the two vaccines are similar. Surrogate virus neutralization test and pseudovirus virus neutralization test further revealed that the single injection vaccine induced strong neutralizing antibody response, with an inhibition equal to that of the corresponding multiple dose vaccine. The vaccine also exhibits good biocompatibility and biosafety. We hope the single dose vaccines like the one developed here will help fighting against highly infectious diseases, e.g., COVID-19.

Declaration of Competing Interest

The authors declare that they have no known competing financial interests or personal relationships that could have appeared to influence the work reported in this paper.

Acknowledgments

We thank the National Natural Science Foundation of China for financial support for this work (Grants Nos: 51873091, 52073146, 52033004 and 51625302).

Supplementary materials

Supplementary material associated with this article can be found, in the online version, at doi:10.1016/j.actbio.2022.08.006.

References

[1] C.R.C. Johns Hopkins University, COVID-19 dashboard by the Center for Systems Science and Engineering (CSSE) at Johns Hopkins University (JHU). https://coronavirus.jhu.edu/map.html (accessed march 7, 2022).
[2] S. Soleimanpour, A. Yaghoubi, COVID-19 vaccine: where are we now and where should we go? Expert Rev. Vaccines 20 (1) (2021) 23–44.
[3] J.Y. Chung, M.N. Thone, Y.J. Kwon, COVID-19 vaccines: the status and perspectives in delivery points of view, Adv. Drug Deliver. Rev. 170 (2021) 1–25.
[4] M.D. Shin, S. Shukla, Y.H. Chung, V. Beiss, S.K. Chan, O.A. Ortega-Rivera, D.M. Wirth, A. Chen, M. Sack, J.K. Pokorski, N.F. Steinmetz, COVID-19 vaccine development and a potential nanomaterial path forward, Nat. Nanotechnol. 15 (8) (2020) 646–655.
[5] J.G. Liang, D. Su, T. Song, Y. Zeng, W. Huang, J. Wu, R. Xu, P. Luo, X. Yang, X. Zhang, S. Luo, Y. Liang, X. Li, J. Huang, Q. Wang, X. Huang, Q. Xu, M. Luo, A. Huang, D. Luo, C. Zhao, F. Yang, J. Han, Y. Zheng, P. Liang, S-Trimer, a

COVID-19 subunit vaccine candidate, induces protective immunity in nonhuman primates, Nat. Commun. 12 (1) (2021) 1346.
[6] J.H. Lam, A.K. Khan, T.A. Cornell, T.W. Chia, R.J. Dress, W.W.W. Yeow, N.K. Mohd-Ismail, S. Venkataraman, K.T. Ng, Y. Tan, D.E. Anderson, F. Ginhoux, M. Nallani, Polymersomes as stable nanocarriers for a highly immunogenic and durable SARS-CoV-2 spike protein subunit vaccine, ACS Nano. 15 (10) (2021) 15754–15770.
[7] Y. Wang, L. Wang, H. Cao, C. Liu, SARS-CoV-2 S1 is superior to the RBD as a COVID-19 subunit vaccine antigen, J. Med. Virol. 93 (2) (2021) 892–898.
[8] L. Liu, Z. Liu, H. Chen, H. Liu, Q. Gao, F. Cong, G. Gao, Y. Chen, Subunit nanovaccine with potent cellular and mucosal immunity for COVID-19, ACS Appl. Bio Mater. 3 (9) (2020) 5633–5638.
[9] Y. Wang, Y. Xie, J. Luo, M. Guo, X. Hu, X. Chen, Z. Chen, X. Lu, L. Mao, K. Zhang, L. Wei, Y. Ma, R. Wang, J. Zhou, C. He, Y. Zhang, Y. Zhang, S. Chen, L. Shen, Y. Chen, N. Qiu, Y. Liu, Y. Cui, G. Liao, Y. Liu, C. Chen, Engineering a self-navigated MnARK nanovaccine for inducing potent protective immunity against novel coronavirus, Nano Today 38 (2021) 101139.
[10] P.S. Arunachalam, A.C. Walls, N. Golden, C. Atyeo, S. Fischinger, C. Li, P. Aye, M.J. Navarro, L. Lai, V.V. Edara, K. Röltgen, K. Rogers, L. Shirreff, D.E. Ferrell, S. Wrenn, D. Pettie, J.C. Kraft, M.C. Miranda, E. Kepl, C. Sydeman, N. Brunette, M. Murphy, B. Fiala, L. Carter, A.G. White, M. Trisal, C. Hsieh, K. Russell-Lodrigue, C. Monjure, J. Dufour, S. Spencer, L. Doyle-Meyers, R.P. Bohm, N.J. Maness, C. Roy, J.A. Plante, K.S. Plante, A. Zhu, M.J. Gorman, S. Shin, X. Shen, J. Fontenot, S. Gupta, D.T. O Hagan, R. Van Der Most, R. Rappuoli, R.L. Coffman, D. Novack, J.S. McLellan, S. Subramaniam, D. Montefiori, S.D. Boyd, J.L. Flynn, G. Alter, F. Villinger, H. Kleanthous, J. Rappaport, M.S. Suthar, N.P. King, D. Veesler, B. Pulendran, Adjuvanting a subunit COVID-19 vaccine to induce protective immunity, Nature 594 (7862) (2021) 253–258.
[11] E.C. Gale, A.E. Powell, G.A. Roth, E.L. Meany, J. Yan, B.S. Ou, A.K. Grosskopf, J. Adamska, V.C.T.M. Picece, A.I. D'Aquino, B. Pulendran, P.S. Kim, E.A. Appel, Hydrogel-based slow release of a receptor-binding domain subunit vaccine elicits neutralizing antibody responses against SARS-CoV-2, Adv. Mater. 33 (51) (2021) 2104362.
[12] X. Qi, B. Ke, Q. Feng, D. Yang, Q. Lian, Z. Li, L. Lu, C. Ke, Z. Liu, G. Liao, Construction and immunogenic studies of a mFc fusion receptor binding domain (RBD) of spike protein as a subunit vaccine against SARS-CoV-2 infection, Chem. Commun. 56 (61) (2020) 8683–8686.
[13] F. Langellotto, M.O. Dellacherie, C. Yeager, H. Ijaz, J. Yu, C. Cheng, N. Dimitrakakis, B.T. Seiler, M.S. Gebre, T. Gilboa, R. Johnson, N. Storm, S. Bardales, A. Graveline, D. White, C.M. Tringides, M.J. Cartwright, E.J. Doherty, A. Honko, A. Griffiths, D.H. Barouch, D.R. Walt, D.J. Mooney, A modular biomaterial scaffold-based vaccine elicits durable adaptive immunity to subunit SARS-CoV-2 antigens, Adv. Healthc. Mater. 10 (22) (2021) 2101370.
[14] M.T. Aguado, Future approaches to vaccine development: single-dose vaccines using controlled-release delivery systems, Vaccine 11 (5) (1993) 596–597.
[15] K.J. McHugh, R. Guarecuco, R. Langer, A. Jaklenec, Single-injection vaccines: progress, challenges, and opportunities, J. Control. Release 219 (Supplement C) (2015) 596–609.
[16] I. Sadeghi, J. Byrne, R. Shakur, R. Langer, Engineered drug delivery devices to address Global Health challenges, J. Control. Release 331 (2021) 503–514.
[17] L. Shi, M.J. Caulfield, R.T. Chern, R.A. Wilson, G. Sanyal, D.B. Volkin, Pharmaceutical and immunological evaluation of a single-shot hepatitis B vaccine formulated with PLGA microspheres, J. Pharm. Sci.-US. 91 (4) (2002) 1019–1035.
[18] K.J. McHugh, T.D. Nguyen, A.R. Linehan, D. Yang, A.M. Behrens, S. Rose, Z.L. Tochka, S.Y. Tzeng, J.J. Norman, A.C. Anselmo, X. Xu, S. Tomasic, M.A. Taylor, J. Lu, R. Guarecuco, R. Langer, A. Jaklenec, Fabrication of fillable microparticles and other complex 3D microstructures, Science 357 (6356) (2017) 1138–1142.
[19] R. Guarecuco, J. Lu, K.J. McHugh, J.J. Norman, L.S. Thapa, E. Lydon, R. Langer, A. Jaklenec, Immunogenicity of pulsatile-release PLGA microspheres for single-injection vaccination, Vaccine 36 (22) (2018) 3161–3168.
[20] C. Korupalli, W. Pan, C. Yeh, P. Chen, F. Mi, H. Tsai, Y. Chang, H. Wei, H. Sung, Single-injecting, bioinspired nanocomposite hydrogel that can recruit host immune cells *in situ* to elicit potent and long-lasting humoral immune responses, Biomaterials 216 (2019) 119268.
[21] Y. Guan, S.G. Yang, Y.J. Zhang, J. Xu, C.C. Han, N.A. Kotov, Fabry-Perot fringes and their application to study the film growth, chain rearrangement, and erosion of hydrogen-bonded PVPON/PAA films, J. Phys. Chem. B 110 (27) (2006) 13484–13490.
[22] Y. Guan, Y. Zhang, Dynamically bonded layer-by-layer films: dynamic properties and applications, J. Appl. Polym. Sci. 131 (19) (2014) 40918.
[23] Y. Zhao, Q. Yuan, C. Li, Y. Guan, Y. Zhang, Dynamic layer-by-layer films: a platform for zero-order release, Biomacromolecules 16 (7) (2015) 2032–2039.
[24] J. Tian, R. Xu, H. Wang, Y. Guan, Y. Zhang, Precise and tunable time-controlled drug release system using layer-by-layer films as erodible coatings, Mater. Sci. Eng. C 116 (2020) 111244.
[25] H. Wang, R. Liu, S. Wang, Y. Guan, Y. Zhang, A highly programmable platform for sequential release of protein therapeutics, J. Mater. Chem. B 9 (6) (2021) 1616–1624.
[26] D.V. Volodkin, N.I. Larionova, G.B. Sukhorukov, Protein encapsulation via porous $CaCO_3$ microparticles templating, Biomacromolecules 5 (5) (2004) 1962–1972.
[27] Y.J. Zhang, Y. Guan, S.G. Yang, J. Xu, C.C. Han, Fabrication of hollow capsules based on hydrogen bonding, Adv. Mater. 15 (10) (2003) 832–835.
[28] Y. Zhao, J. Gu, S. Jia, Y. Guan, Y. Zhang, Zero-order release of polyphenolic drugs from dynamic, hydrogen-bonded LBL films, Soft Matter 12 (4) (2016) 1085–1092.
[29] Z. Wang, M. Fu, Y. Wang, Q. Meng, Y. Guan, Y. Zhang, An injectable carrier for zero-order release of salmon calcitonin, ACS Biomater. Sci. Eng. 6 (1) (2020) 485–493.
[30] Y. Wang, M. Fu, Z. Wang, J.X.X. Zhu, Y. Guan, Y. Zhang, Sustained zero-order release carrier for long-acting, peakless basal insulin therapy, J. Mater. Chem. B 8 (9) (2020) 1952–1959.
[31] M. Fu, X. Zhuang, T. Zhang, Y. Guan, Q. Meng, Y. Zhang, Hydrogen-bonded films for zero-order release of leuprolide, Macromol. Biosci. 20 (9) (2020) 2000050.
[32] N. Wen, Y. Dong, R. Song, W. Zhang, C. Sun, X. Zhuang, Y. Guan, Q. Meng, Y. Zhang, Zero-order release of gossypol improves its antifertility effect and reduces its side effects simultaneously, Biomacromolecules 19 (6) (2018) 1918–1925.
[33] Y. Zhao, X. Xu, N. Wen, R. Song, Q. Meng, Y. Guan, S. Cheng, D. Cao, Y. Dong, J. Qie, K. Liu, Y. Zhang, A drug carrier for sustained zero-order release of peptide therapeutics, Sci. Rep. 7 (1) (2017) 5524.
[34] E. Kim, G. Erdos, S. Huang, T.W. Kenniston, S.C. Balmert, C.D. Carey, V.S. Raj, M.W. Epperly, W.B. Klimstra, B.L. Haagmans, E. Korkmaz, L.D. Falo, A. Gambotto, Microneedle array delivered recombinant coronavirus vaccines: Immunogenicity and rapid translational development, EBioMedicine 55 (2020) 102743.
[35] J. Jia, Q. Liu, T. Yang, L. Wang, G. Ma, Facile fabrication of varisized calcium carbonate microspheres as vaccine adjuvants, J. Mater. Chem. B. 5 (8) (2017) 1611–1623.
[36] P.A. Darrah, D.T. Patel, P.M. De Luca, R.W.B. Lindsay, D.F. Davey, B.J. Flynn, S.T. Hoff, P. Andersen, S.G. Reed, S.L. Morris, M. Roederer, R.A. Seder, Multifunctional TH1 cells define a correlate of vaccine-mediated protection against Leishmania major, Nat. Med. 13 (7) (2007) 843–850.
[37] C.W. Tan, W.N. Chia, X. Qin, P. Liu, M.I.C. Chen, C. Tiu, Z. Hu, V.C. Chen, B.E. Young, W.R. Sia, Y. Tan, R. Foo, Y. Yi, D.C. Lye, D.E. Anderson, L. Wang, A SARS-CoV-2 surrogate virus neutralization test based on antibody-mediated blockage of ACE2–spike protein–protein interaction, Nat. Biotechnol. 38 (9) (2020) 1073–1078.